Int. J. Electrochem. Sci., 9 **(2014)** 5164 - 5176

International Journal of
ELECTROCHEMICAL
SCIENCE
www.electrochemsci.org

Berberine as an Effective Corrosion Inhibitor for 7075 Aluminium Alloy in 3.5% NaCl Solution

Ambrish Singh[1,2], *Yuanhua Lin*[1,*], *Wanying Liu*[1], *Jie Pan*[3], *Chengqiang Ren*[4], *Dezhi Zeng*[1], *Shijie Yu*[4]

[1] State Key Laboratory of Oil and Gas Reservoir Geology and Exploitation (Southwest Petroleum University), Chengdu, Sichuan 610500, China.
[2] Department of Chemistry, School of Civil Engineering, LFTS, Lovely Professional University, Phagwara, Punjab 144402, India.
[3] CNPC Key Lab for Tubular Goods Engineering (Southwest Petroleum University), Chengdu, Sichuan 610500, China.
[4] School of Material Science and Engineering (Southwest Petroleum University), Chengdu, Sichuan 610500, China.
[*]E-mail: yhlin28@163.com

Received: 23 February 2014 / *Accepted:* 5 June 2014 / *Published:* 16 June 2014

The inhibition behavior of 5,6-dihydro-9,10-dimethoxybenzo[g]-1,3-benzodioxolo[5,6-a]quinolizinium (berberine) as an environment-benign corrosion inhibitor for AA7075 aluminium alloy was investigated in 3.5 wt.% NaCl solution by means of potentiodynamic polarization, AC impedance, scanning electrochemical spectroscopy (SECM) and scanning electron microscopy (SEM). The results showed that berberine can inhibit the corrosion of 7075 al alloy at different immersion time. The surface analysis also revealed the retardation of corrosion due to adsorption of inhibitor molecules on the al alloy surface.

Keywords: Aluminium alloy; SECM; SEM; Corrosion; Inhibition

1. INTRODUCTION

Aluminium alloys have recently attracted more and more attention for their high strength-to-density ratio, the wrought aluminum-zinc-magnesium-copper AA7075 series alloys are commonly used in the transport applications, aviation industry, bicycle components, rock climbing equipment, inline skating-frames, and hang glider airframes [1-5]. It has become an important topic to improve the corrosion resistance of aluminium alloys concerning practical applications of Al alloys in industry. Aluminum has natural corrosion protection from its oxide layer but if exposed to aggressive

environments it may corrode. Especially in the presence of chloride ions (Cl^-), such as in seawater, the oxide layer is broken down.

Use of corrosion inhibitors is the most common method used to retard corrosion of metals as no special equipments required, low cost, and easy operation. Overall, many corrosion inhibitors have some health and/or environmental problems due to their toxicity. It is highly desired that new inhibitors for Al are non-toxic and environment-friendly. Use of different parts of plant as corrosion inhibitor is in practice nowadays as they are renewable, cheap, easily available and non toxic. Many amines, steroids, and alkaloids are derived from the plants, which are rich in heteroatoms (N, O, S). Literature survey has concluded that compounds containing heteroatoms show good inhibition [6-8].

In present study we have used root extract of *Coptis chinensis*, which is a native plant of China to extract an isoquinoline alkaloid dye named berberine as shown in Fig. 1. We extracted berberine a yellow dye from the root, which is rich in heteroatoms and has also been commonly used as a non-toxic antibiotic for years in China. It is the only cationic dye among the natural plant dyes that is part of the chemical group of isoquinoline alkaloids [9].

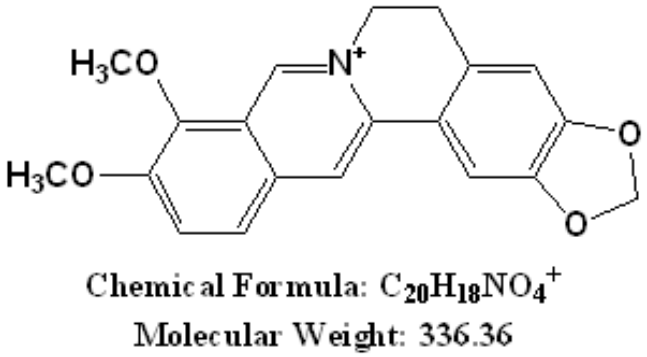

Figure 1. Berberine- IUPAC name (5,6-dihydro-9,10-dimethoxybenzo[g]-1,3-benzodioxolo[5,6-a]quinolizinium).

2. EXPERIMENTAL

2.1. Preparation of inhibitor

The roots of the *Coptis chinensis* plant were collected from the field, and the roots were dried and powdered for extraction. Fifty grams of the powder was soaked in 900 ml of reagent grade ethanol for 24 h and refluxed for 5 h. The ethanolic solution was filtered and concentrated to 500 ml. This extract was used to study the corrosion inhibition properties.

2.2. Materials and Solutions

Aluminium 7075 alloy with density 2.83 g/cm^3 having following composition (wt %): Si 0.41; Cu 1.38; Mg 2.62; Zn 5.89; Mn $\leq$ 0.30; Ti $\leq$ 0.20; Fe 0.50 and balance Al were used for all studies.

Aluminium alloy coupons having dimensions of 30 mm × 3 mm × 3 mm were used for the electrochemical study. The specimens were metallographically polished according to ASTM A262, degreased, and dried before experiment. The test solution of 3.5% NaCl was prepared by analytical grade NaCl with double distilled water. We did some preliminary electrochemical tests to obtain the optimum concentration of the inhibitor. After the tests optimum concentration was found to be 1000 ppm as after this no significant change was observed in the results. And this concentration of inhibitor was used for further studies.

2.3. Electrochemical measurements

The electrochemical experiments were performed by using three electrode cell, connected to Potentiostat/Galvanostat CHI604D. Zview software package was used for data fitting. Aluminium alloy was used as working electrode, platinum electrode as an auxiliary electrode, and saturated calomel electrode (SCE) as reference electrode. Tafel curves were obtained at a scan rate of 1.0 mVs^{-1}. EIS measurements were performed under potentiostatic conditions in a frequency range from 100 kHz to 0.01 Hz, with amplitude of 10 mV AC signal. The experiments were carried out when the electrochemical system was in steady state.

2.4. Surface Analysis

2.4.1. Scanning Electrochemical Microscopy (SECM)

A model of scanning electrochemical microscopy CHI900C was used. The instrument was operated with a 10 μm platinum tip as the probe, an Ag/AgCl/KCl (saturated) reference electrode and a platinum counter electrode to test the samples at different immersion time. All potential values are referred to the Ag/AgCl/KCl (saturated) reference electrode. The measurements of line scans were generated with the tip at ~ 10 μm from the specimen surface in all the cases. The scan rate was 80 μm/step. Scanning electrochemical microscopy (SECM) is a technique in which the current that flows through a very small electrode tip (generally an ultramicroelectrode with a tip diameter of 10 μm or less) near a conductive, semiconductive, or insulating substrate immersed in solution is used to characterize processes and structural features at the substrate as the tip is moved near the surface [18-20]. The tip can be moved normal to the surface (the z direction) to probe the diffusion layer, or the tip can be scanned at constant z across the surface (the x and y directions). The tip and substrate are part of an electrochemical cell that usually also contains other (e.g., auxiliary and reference) electrodes. The diameter of the samples was between 30 × 3 × 3 mm.

2.4.2. Scanning Electron Microscopy (SEM) and Energy-dispersive X-ray spectroscopy (EDX)

Before surface examination, the electrodes were immersed in the test solution (3.5% NaCl) in the absence and presence of corrosion inhibitor to observe the effect of corrosion and inhibition at

different immersion time. The Al alloy electrodes were then dried at ambient temperature. Micrographs of abraded and corroded Al alloy surfaces and those after inhibitor addition were taken using a SEM model Ametek-EDAX TSL for different immersion time. The changes in surface composition were analyzed with an EDX detector module coupled with SEM.

3. RESULTS AND DISCUSSION

3.1. Electrochemical measurements

3.1.1. Potentiodynamic polarization measurements

The corrosion potential (E_{corr}), corrosion current density (I_{corr}), and anodic (β_a) and cathodic (β_C) slopes are obtained by the anodic and cathodic regions of the tafel plots at different immersion time table 1.

Table 1. Tafel polarization data for aluminium alloy in 3.5% NaCl for different immersion time at optimum concentration of berberine.

Solutions	Tafel data				
	I_{corr}	b_a	$-b_c$	η	Surf. Coverage
	(μA cm^{-2})	(mV d^{-1})	(mV d^{-1})	(%)	θ
3.5% NaCl 24 Hr	520	53	92	-	-
Berberine 1000 ppm 24 Hr	94	26	85	81	0.81
3.5% NaCl 48 Hr	470	37	69	-	-
Berberine 1000 ppm 48 Hr	75	34	71	84	0.84
3.5% NaCl 72 Hr	780	15	79	-	-
Berberine 1000 ppm 72 Hr	50	13	81	94	0.94

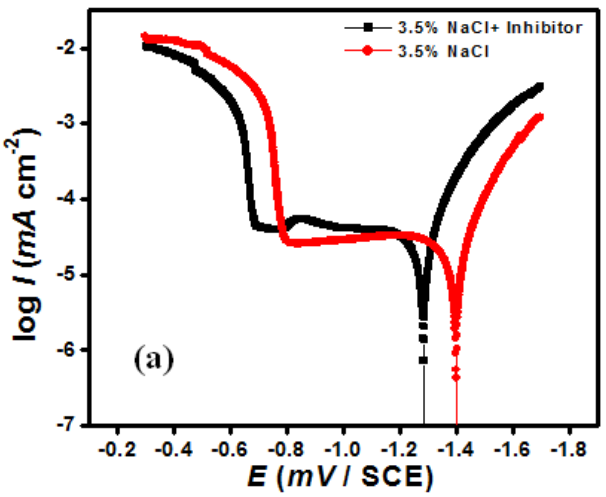

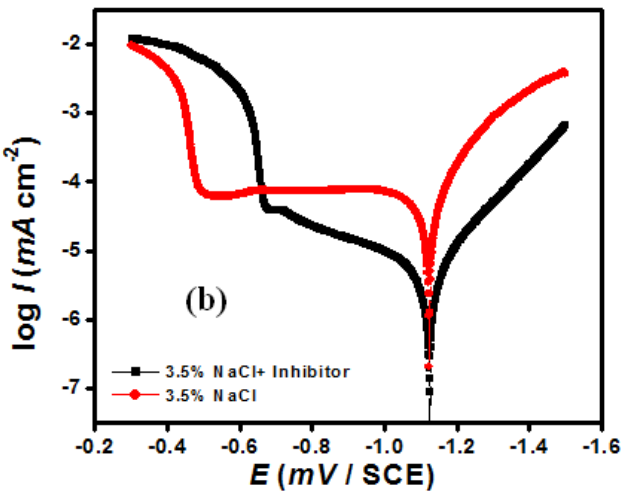

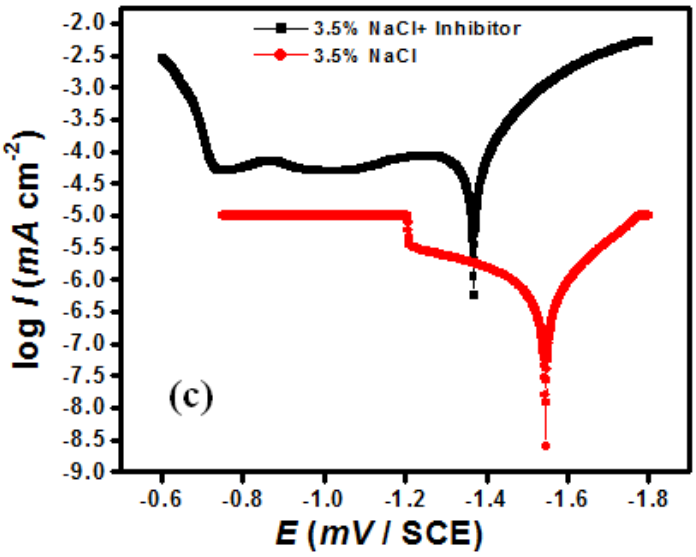

Figure 2. Tafel plots for aluminium alloy in 3.5% NaCl for different immersion time (a) 24 hr (b) 48 hr and (c) 72 hr at optimum concentration of berberine.

The corrosion current density (I_{corr}) can be obtained by extrapolating the tafel lines to the corrosion potential and the inhibition efficiency (η %) values were calculated from the relation:

$$\eta\% = \frac{I_{corr} - I_{corr(i)}}{I_{corr}} \times 100 \quad (1)$$

Where I_{corr} and $I_{corr(i)}$ are the corrosion current density in absence and presence of inhibitor. The polarization curves for aluminium alloy in optimum concentration of inhibitor at different immersion time are given in Fig. 2.

In this case, the cathodic reaction occurring at the aluminium-solution interface is hydrogen evolution. The results show that the cathodic slopes (β_c) are much greater than that expected for H_2 evolution. Such large cathodic Tafel slopes are not unexpected for aluminium, and have previously been reported for H_2 evolution reaction on aluminium electrodes covered probably with an oxide or an oxide-inhibitor complex [10]. So the inhibition of corrosion of aluminium in 3.5% NaCl is under cathodic control. The η% decreases with increasing temperature as indicated in table 1. This is due to increased rate of dissolution process of al alloy and partial desorption of the inhibitor from the metal surface [11-14]. The results showed the decrease in I_{corr} in presence of inhibitor as compared to blank solution at various immersion time intervals. This is due to adsorption of inhibitor on metal surface which penetrates rate of corrosion current density and increases inhibition efficiency as shown in table 2 [15-18]. Thus, we observe the reduction of general corrosion of AA7075 alloy in the 3.5% NaCl solution with the presence and absence of studied inhibitor [19].

3.1.2. Electrochemical Impedance Spectroscopy

Electrochemical impedance spectroscopy measurements were carried out in order to study the kinetics of the electrode process and the surface properties of the studied system at various immersion

times. This method is widely used to investigate the corrosion inhibition process [20-22] Nyquist plots of aluminium alloy in 3.5% NaCl solution in optimum concentration of berberine at immersion time are shown in Fig. 4. A high frequency depressed charge transfer semicircle is observed. Such behavior is characteristic for solid electrodes and is often referred to as a frequency dispersion effect, which can be imputed to non homogeneity and the rough-textured metal surface. The inductive loop may be a consequence of the layer stabilization byproducts of the corrosion reaction on the electrode involving inhibitor molecules and their reactive products [23-25]. It is clear from Fig. 4 that the impedance spectra corresponds to surface heterogeneity which may be the result of surface roughness, dislocation, distribution of active sites, or adsorption of the different berberine molecules [26-30].

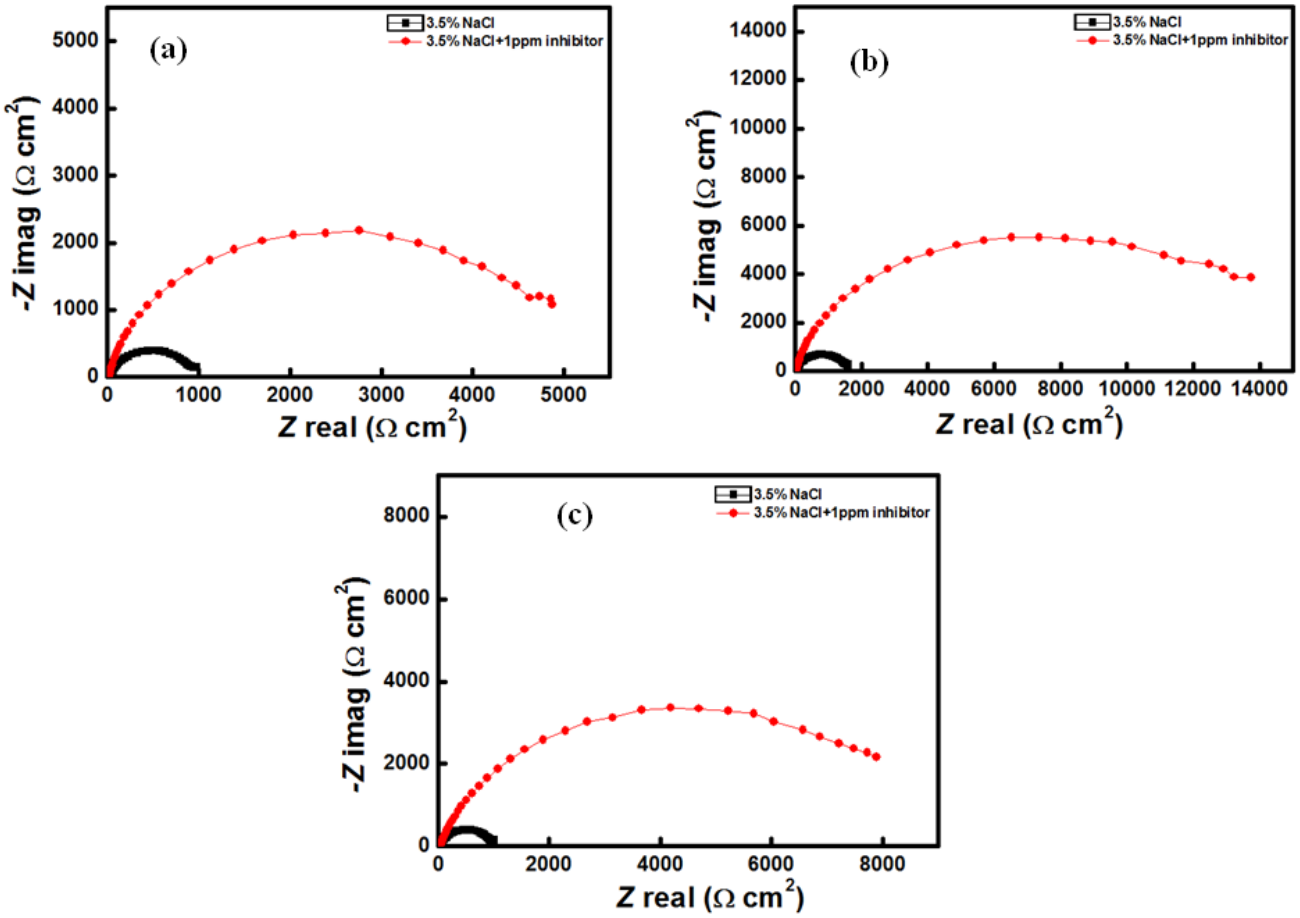

Figure 3. Nyquist plots for aluminium alloy in 3.5% NaCl for different immersion time (a) 24 hr (b) 48 hr and (c) 72 hr at optimum concentration of berberine.

The model used for fitting consist the solution resistance (*R*s), the charge-transfer resistance of the interfacial corrosion reaction (*R*ct) and the constant phase angle element (CPE) [31, 32].

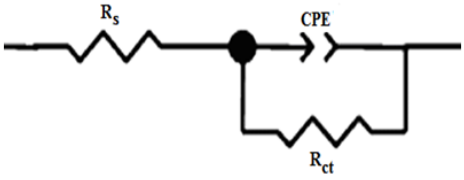

The inhibition efficiency is calculated using charge transfer resistance (R_{ct}) as follows,

$$\eta\% = \frac{R_{ct(inh)} - R_{ct}}{R_{ct(inh)}} \times 100 \quad (6)$$

Where $R_{ct(inh)}$ and R_{ct} are the values of charge transfer resistance in presence and absence of inhibitor in 3.5% NaCl respectively. At different immersion time berberine showed increase in value of R_{ct} with respect to blank 3.5% NaCl solution as shown in table 2. The increase in R_{ct} values is attributed to the increase in resistance and adsorption of inhibitor molecules on aluminium alloy surface [33-36].

Table 2. Nyquist data for aluminium alloy in 3.5% NaCl for different immersion time at optimum concentration of berberine.

Solutions	Conc.(ppm)	R_s (Ω cm^2)	R_{ct} (Ω cm^2)	η%	θ	n
	-	2.5	981	-	-	0.827
Berberine 24 Hr	1000 ppm	1.7	5148	80	0.80	0.885
3.5% NaCl 48 Hr	-	2.8	1655	-	-	0.849
Berberine 48 Hr	1000 ppm	2.6	13726	87	0.87	0.875
3.5% NaCl 72 Hr	-	2.7	1020	-	-	0.804
Berberine 72 Hr	1000 ppm	1.7	9085	88	0.88	0.811

3.2. Surface Analysis

3.2.1. SECM

The scanning electrochemical microscope (SECM) [37] has been introduced to the corrosion field, giving valuable microscopic information from a corroding surface [38], allowing the measurement of local differences in electrochemical reactivity. The important advantage of the SECM technique is that it operates on both insulating (coated / films) and conducting (non-coated) surfaces, thus allowing one to easily distinguish between the coated and corroded surfaces [39, 40].

Prior to each SECM scanning experiment; the tip-sample distance was established by approach curves performed above the insulating part of the coating at -0.70 V. The status of a corroded sample was studied by monitoring the probe (tip potential: 0.5 V vs Ag/AgCl/saturated KCl reference electrode) and the substrate (tip potential: -0.7 V) in test solutions. Corrosion activity is observed from 10 minutes after immersion in the electrolyte solution.

Fig. 4a-l presents the morphology of the specimens visualized by scanning electrochemical microscope for different immersion time. However, when an insulating surface (having film or coating) as we used berberine with 3.5% NaCl solution is approached in an SECM measurement the diffusion field surrounding the tip is hindered and the tip current decreases. On the contrary, an increase in the current is observed when a conductor blank 3.5% NaCl solution without berberine is approached, because the redox mediator is regenerated at the surface.

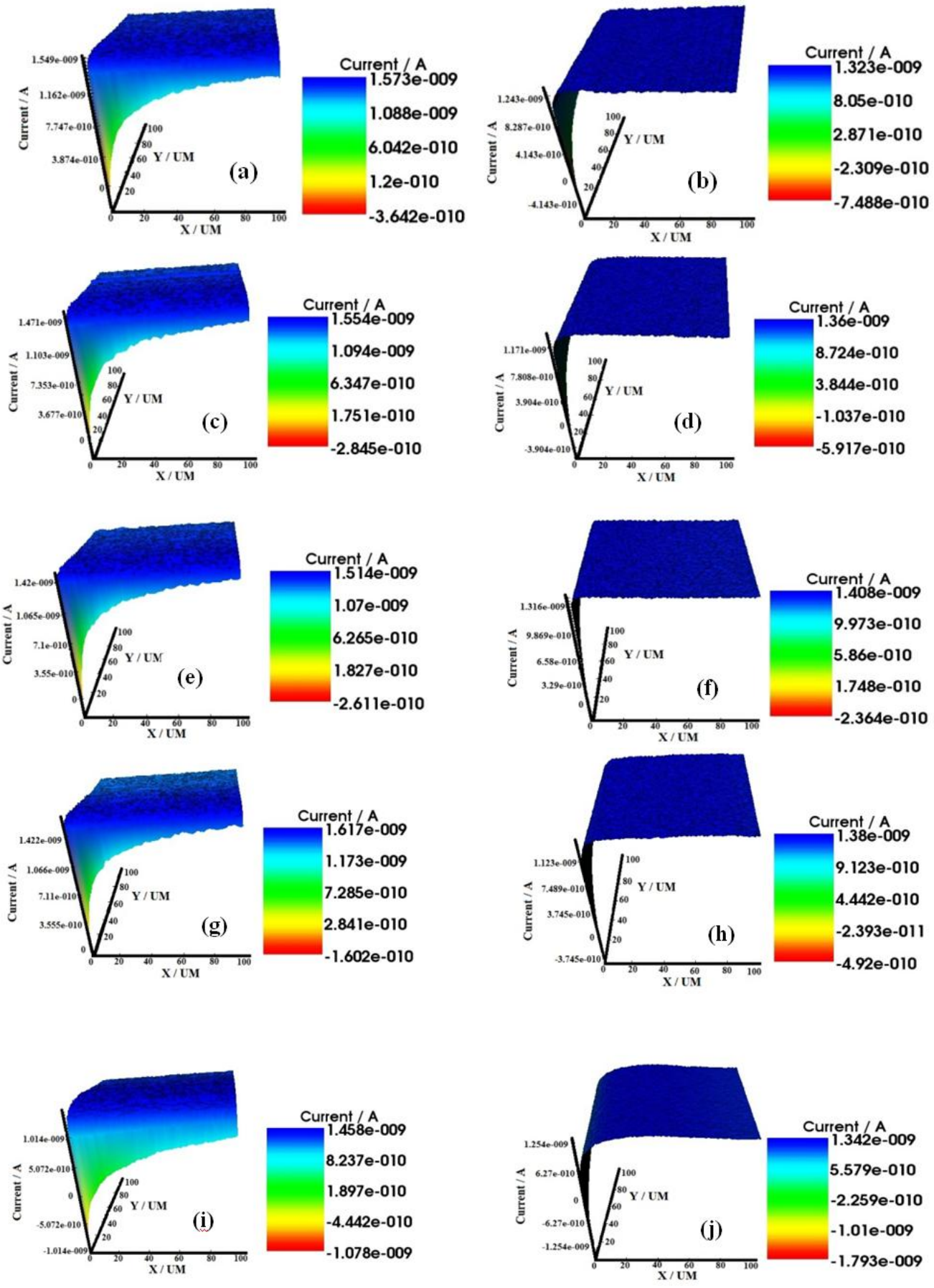
(a)
Current / A
1.573e-009
1.088e-009
6.042e-010
1.2e-010
-3.642e-010
1.549e-009
1.162e-009
7.747e-010
3.874e-010
0
Current / A
Y / UM
X / UM
(b)
Current / A
1.323e-009
8.05e-010
2.871e-010
-2.309e-010
-7.488e-010
1.243e-009
8.287e-010
4.143e-010
0
-4.143e-010
Y / UM
X / UM
(c)
Current / A
1.554e-009
1.094e-009
6.347e-010
1.751e-010
-2.845e-010
1.471e-009
1.103e-009
7.353e-010
3.677e-010
0
Y / UM
X / UM
(d)
Current / A
1.36e-009
8.724e-010
3.844e-010
-1.037e-010
-5.917e-010
1.171e-009
7.808e-010
3.904e-010
0
-3.904e-010
Y / UM
X / UM
(e)
Current / A
1.514e-009
1.07e-009
6.265e-010
1.827e-010
-2.611e-010
1.42e-009
1.065e-009
7.1e-010
3.55e-010
0
Y / UM
X / UM
(f)
Current / A
1.408e-009
9.973e-010
5.86e-010
1.748e-010
-2.364e-010
1.316e-009
9.869e-010
6.58e-010
3.29e-010
0
Y / UM
X / UM
(g)
Current / A
1.617e-009
1.173e-009
7.285e-010
2.841e-010
-1.602e-010
1.422e-009
1.066e-009
7.11e-010
3.555e-010
0
Y / UM
X / UM
(h)
Current / A
1.38e-009
9.123e-010
4.442e-010
-2.393e-011
-4.92e-010
1.123e-009
7.489e-010
3.745e-010
0
-3.745e-010
Y / UM
X / UM
(i)
Current / A
1.458e-009
8.237e-010
1.897e-010
-4.442e-010
-1.078e-009
1.014e-009
5.072e-010
0
-5.072e-010
-1.014e-009
Y / UM
X / UM
(j)
Current / A
1.342e-009
5.579e-010
-2.259e-010
-1.01e-009
-1.793e-009
1.254e-009
6.27e-010
0
-6.27e-010
-1.254e-009
Y / UM
X / UM

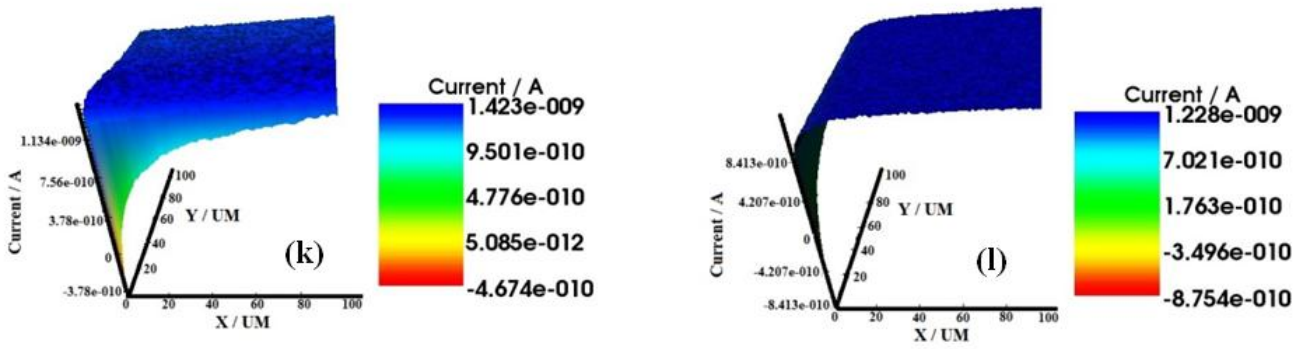

Figure 4. SECM images of (a) Blank x-axis after 24 hr 3-D view (b) Blank y-axis after 24 hr 3-D view (c) Inhibited x-axis after 24 hr 3-D view (d) Inhibited y-axis after 24 hr 3-D view (e) Blank x-axis after 48 hr 3-D view (f) Blank after 48 hr 3-D view (g) Inhibited x-axis after 48 hr 3-D view (h) Inhibited y-axis after 48 hr 3-D view (i) Blank x-axis after 72 hr 3-D view (j) Blank y-axis after 72 hr 3-D view (k) Inhibited x-axis after 72 hr 3-D view (l) Inhibited y-axis after 72 hr 3-D view.

SECM images in Fig. 4a, 4b, 4e, 4f, 4i and 4j showed the blank (3.5% NaCl solution) x-axis and y-axis 3D view while 4c, 4d, 4g, 4h, 4k, and 4l revealed the presence of inhibitor the x-axis and y-axis 3D view at different immersion time.

In the absence of berberine the aluminium alloy surface remains conductive, which are evidenced by an increase in current as the surface is approached as shown in Fig. 4. When berberine has been added to the solution a gradual transition from a conducting to an insulating surface is seen. Comparing the currents across the corroded sample and the specimens incorporated with inhibitor solution, the protection effect of the inhibitor adsorbed on the specimen surface can be justified [41].

3.2.2. SEM-EDX

To establish whether the corrosion inhibition is due to the formation of an adsorptive film on the Al alloy, scanning electron photographs were taken (Fig. 5a-f) for different immersion time.

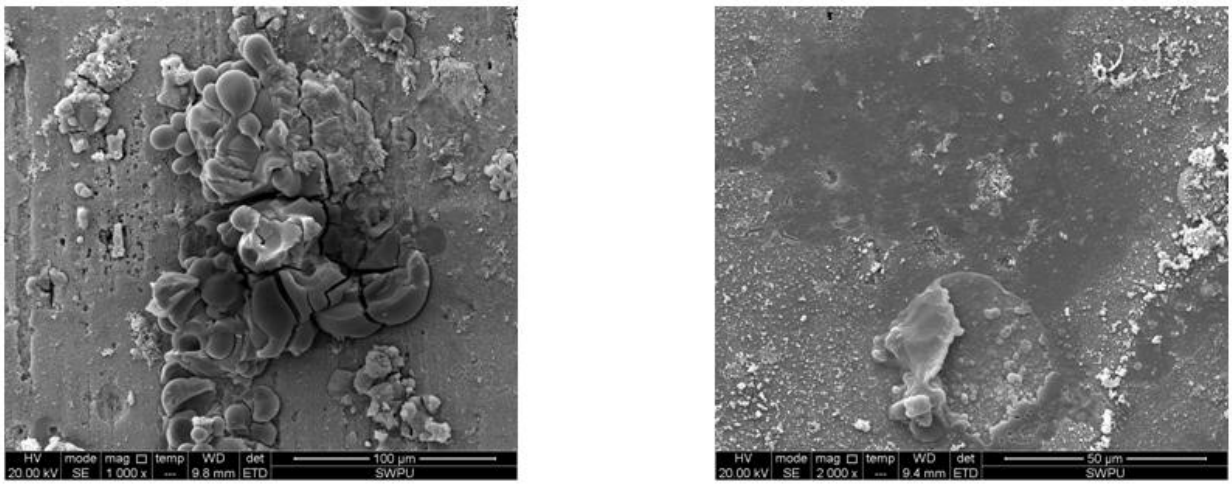

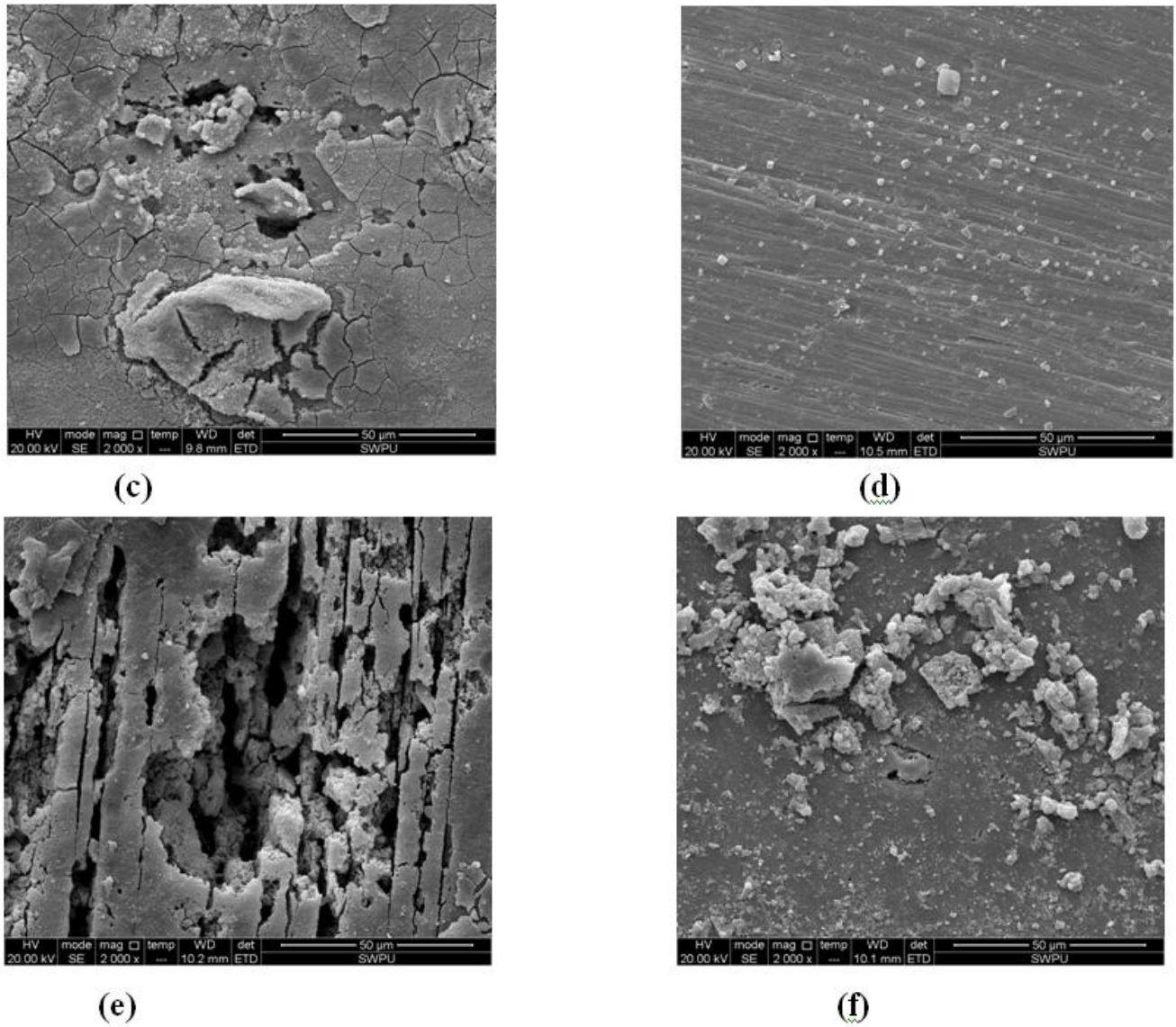

Figure 5. SEM micrographs of al alloy surfaces: (a) Blank at 24 hr (b) Inhibited at 24 hr (c) Blank at 48 hr (d) Inhibited at 48 hr (e) Blank at 72 hr (f) Inhibited at 72 hr at optimum concentration of berberine.

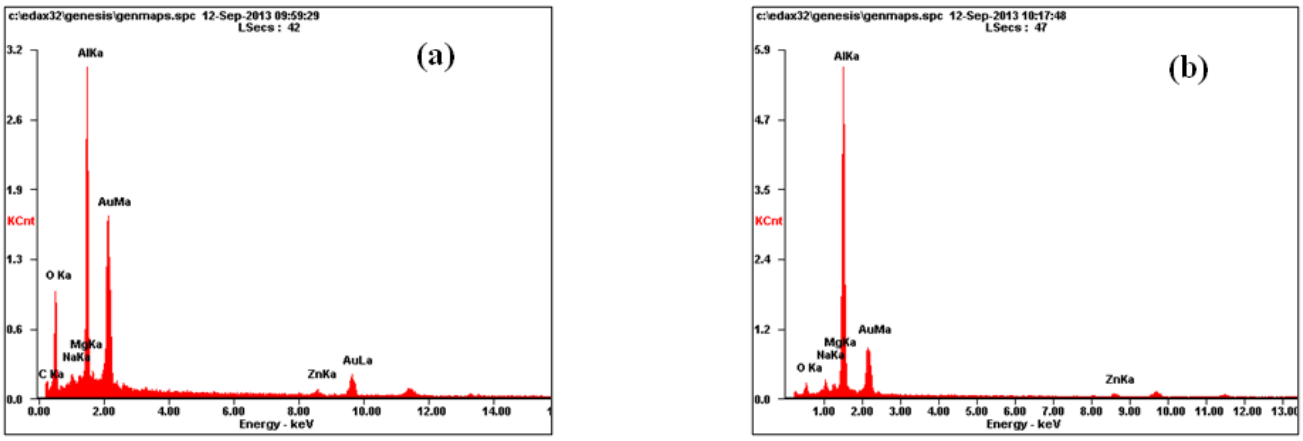

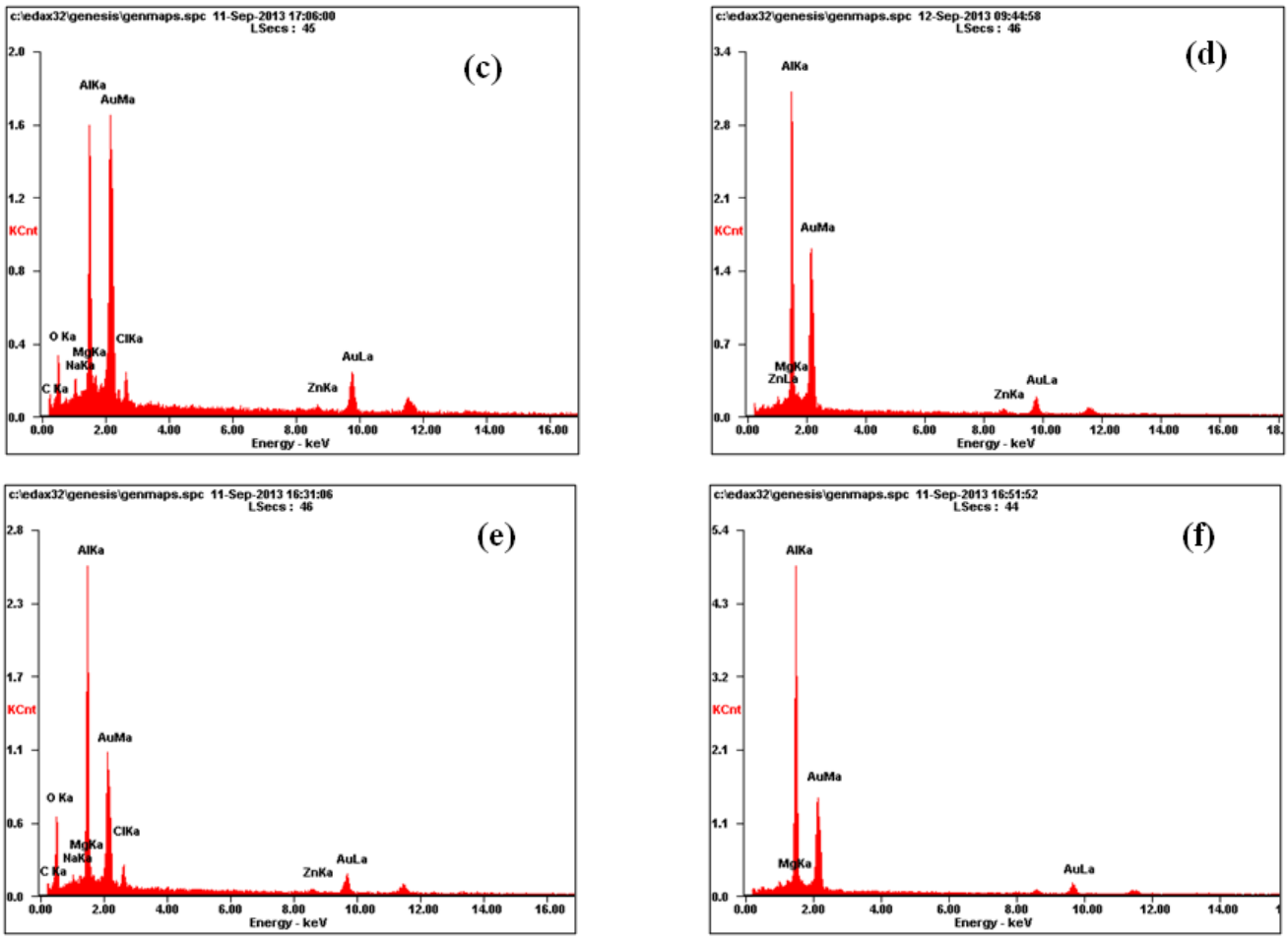

Figure 6. EDX spectra of al alloy surfaces: (a) Blank at 24 hr (b) Inhibited at 24 hr (c) Blank at 48 hr (d) Inhibited at 48 hr (e) Blank at 72 hr (f) Inhibited at 72 hr at optimum concentration of berberine.

Fig. 5a after 24 hr, 5c after 48 hr and 5e after 72 hr showed a rough and perished surface in 3.5% NaCl solution while in presence of berberine (Fig. 5b, 5d and 5f) the surface was less corroded and smooth. Therefore, a smooth and much less corroded morphology of Al alloy samples results from exposure to the inhibitor solutions. These results prove that the berberine can effectively protect Al alloy samples from a corrosive environment. The specimen in the presence of berberine shows comparatively less corrosion and a smooth surface, indicating its strong protective film on the electrode surface.

EDX spectra were used to determine the elements present on the metal surface before and after exposure to the inhibitor solution. The EDX results are displayed in Fig. 6a-f for different immersion time. Fig. 6a after 24 hr, 6c after 48 hr and 6e after 72 hr are the EDX spectrum of the uninhibited al alloy sample, which indicates the presence of Na and Cl peaks along with Al, Zn, Cr, Mg, which led to the breakdown of the oxide film and free corrosion of bare metal. Spectra of Fig. 6b after 24 hr, 6d after 48 hr and 6f after 72 hr showed that the metal peaks are considerably suppressed relative to the uninhibited al alloy sample. Additional peak of Au is seen in EDX spectra for different immersion time as Gold (Au) was sprayed on the sample for better conductivity with the metal surface. The

suppression of peak occurs because of the overlying inhibitor film on aluminium alloy surface. The EDX analysis confirms the formation of film on the al alloy surface that results in suppressed peaks in presence of the inhibitor.

5. CONCLUSIONS

In this study, corrosion inhibition efficiency of berberine on 7075 aluminium alloy in 3.5% NaCl was determined by electrochemical and surface analysis at different immersion time. Electrochemical impedance spectroscopy data reveals increase in R_{ct} values, which accounted for good inhibition efficiency. The surface studies by SECM and SEM confirmed the blockage of metal surface through adsorption process. All these data support good inhibition tendency of berberine.

ACKNOWLEDGEMENTS
Authors are thankful to the post doctoral fellowship, financial assistance provided by the National Natural Science Foundation of China (No. 51274170) and the research grants from the Colonel Technology Fund of Southwest Petroleum University (Project No.2012XJZ013).

References

1. M. Dabala, E. Ramous, M. Magrini, *Mater. Corros.* 55 (2004) 381-386.
2. P. Cavaliere, *Mater. Charact*. 57 (2006) 100-104.
3. R. Rosliza, W. B. Wan Nik, S. Izman, Y. Prawoto, *Curr. Appl Phys.* 10 (2010) 923-929.
4. J. A. Hill, T. Markley, M. Forsyth, P. C. Howlett, B. R. W. Hinton, *J. Alloys Compd.* 509 (2011) 1683-1690.
5. R. Rosliza, W. B. Wan Nik, H. B. Senin, *Mater. Chem. Phys.* 107 (2008) 281-288.
6. I. B. Obot, N. O. Obi-Egbedi, S. A. Umoren, E. E. Ebenso, *Int. J. Electrochem. Sci.* 5 (2010) 994-1007.
7. A. Y. El-Etre, *Corros. Sci.* 45 (2003) 2485-2495.
8. P. M. Krishnegoweda, V. T. Venkatesha, P. K. M. Krishnegoweda, S. B. Sivayogiraju, *Ind. Eng. Chem. Res.* 52 (2013) 722-728.
9. Y. Li, P. Zhao, Q. Liang, B. Hou, *Appl. Surf. Sci.* 252 (2005) 1245-1253.
10. J. O. M. Bockris, A. K. N. Reddy, M. Gamboa-Aldeco, *Modern Electrochemistry*; Kluwer Academic/ Plenum Publishers: New York, (2000) 862-910.
11. D. K. Yadav, D. S. Chauhan, I. Ahamad, M. A. Quraishi, *RSC Adv.* 3 (2013) 632-646.
12. S. Deng, X. Li, *Corros. Sci.* 55 (2012) 407-415.
13. G. Husnu, S. H. Ibrahim, *Ind. Eng. Chem. Res.* 51 (2012) 785-792.
14. G. Ji, S. K. Shukla, P. Dwivedi, S. Sundaram, R. Prakash, *Ind. Eng. Chem. Res.* 50 (2011) 11954-11959.
15. M. A. Chidiebere, C. E. Ogukwe, K. L. Oguzie, C N. Eneh, E. E. Oguzie, *Ind. Eng. Chem. Res.* 51 (2012) 668-677.
16. E. E. Oguzie, K. L. Oguzie, C. O. Akalezi, I. O. Udeze, J. N. Ogbulie, V. O. Njoku, *ACS Sustainable Chem. Eng.* 1 (2013) 214-225.
17. P. B. Raja, M. G. Sethuraman, *Mater. Lett.* 62 (2008) 2977-2979.

18. M. A. Quraishi, A. Singh, V. K. Singh, D. K. Yadav, A. K. Singh, *Mater. Chem. Phys.* 122 (2010) 114-122.
19. E. M. Sherif, *Int. J. Electrochem. Sci.* 6 (2011) 1479-1492.
20. A. Singh, E. E. Ebenso, M. A. Quraishi, *Int. J. Electrochem. Sci.* 7 (2012) 3409-3419.
21. A. Singh, I. Ahamad, M. A. Quraishi, *Arab. J. Chem.* (2013) http://dx.doi.org/10.1016/j.arabjc.2012.04.029.
22. I. Ahamad, R. Prasad, M. A. Quraishi, *J. Solid State Electrochem.* 14 (2010) 2095-2105.
23. K. F. Khaled, *Electrochim. Acta.* 54 (2009) 6523-6532.
24. T. Poornima, J. Nayak, A. N. Shetty, *Corros. Sci.* 53 (2011) 3688-3696.
25. R. Solmaz, G. Kardas, M. Culha, B. Yazici, M. Erbil, *Electrochim. Acta.* 53 (2008) 5941-5952.
26. Y. Abboud, A. Abourriche, T. Ainane, M. Charrouf, A. Bennamara, O. Tanane, B. Hammouti, *Chem. Eng. Commun.* 196 (2009) 788-800.
27. A. Singh, I. Ahamad, V. K. Singh, M. A. Quraishi, *J. Solid State Electrochem.* 15 (2011) 1087-1097.
28. M. Lebrini, F. Robert, A. Lecante, C. Roos, *Corros. Sci.* 53 (2011) 687-695.
29. A. Khamis, M. M. Saleh, M. I. Awad, *Corros. Sci.* 66 (2013) 343-349.
30. P. B. Raja, A. K. Qureshi, A. A. Rahim, H. Osman, K. Awang, *Corros. Sci.* 69 (2013) 292-301.
31. A. Lecante, F. Robert, P. A. Blandinières, C. Roos, *Curr. Appl. Phys.* 11 (2011) 714-724.
32. A. Yurt, S. Ulutas, H. Dat, *Appl. Surf. Sci.* 253 (2006) 919-925.
33. C. Kamal, M. G. Sethuraman, *Ind. Eng. Chem. Res.* 51 (2012) 10399-10407.
34. I. B. Obot, N. O. Obi-Egbedi, S. A. Umoren, *Corros. Sci.* 51 (2009) 276-282.
35. M. Lashgari, A. M. Malek, *Electrochim. Acta.* 55 (2010) 5253-5257.
36. I. B. Obot, N. O. Obi-Egbedi, S. A. Umoren, E. E. Ebenso, *Int. J. Electrochem. Sci.* 5 (2010) 994-1007.
37. A. J. Bard, F. R. F. Fan, J. Kwak, O. Lev, *Anal. Chem.* 61 (1989) 132-138.
38. C. Lee, A. J. Bard, *Anal. Chem.* 62 (1990) 1906 -1913.
39. Bard, A. J.; Denuault, G.; Lee, C.; Mandler, D.; Wipf, D. O. *Acc. Chem. Res.* 1990 23 357-363.
40. B. M. Quinn, I. Prieto, S. K. Haram, A. J. Bard, *J. Phys. Chem. B.* 105 (2001) 7474-7476.
41. M. Tsionsky, A. J. Bard, D. Dini, F. Decker, *Chem. Mater.* 10 (1998) 2120-2126.